

1,25(OH)₂D₃ inhibits high glucose-induced apoptosis and ROS production in human peritoneal mesothelial cells via the MAPK/P38 pathway

LINA YANG^{1,2}, LAN WU², SHUYAN DU³, YE HU¹, YI FAN¹ and JIANFEI MA¹

Departments of ¹Nephrology, ²Geriatrics and ³Central Laboratory,
The First Affiliated Hospital, China Medical University, Shenyang, Liaoning 110001, P.R. China

Received July 3, 2015; Accepted April 26, 2016

DOI: 10.3892/mmr.2016.5323

Abstract. The regulation of cell proliferation, differentiation and immunomodulation are affected by 1,25(OH)₂D₃. However, its function during apoptosis and oxidative stress in human peritoneal mesothelial cells (HPMCs) remains unknown. The aim of the present study was to investigate whether the regulation of apoptosis and oxidative stress have therapeutic relevance in peritoneal dialysis (PD) therapy. The present study investigated the effects of 1,25(OH)₂D₃ on high glucose (HG)-induced apoptosis and reactive oxygen species (ROS) production in HPMCs, and examined the underlying molecular mechanisms. Flow cytometry and western blotting were performed to detect cell apoptosis, 2,7-dichlorofluorescein diacetate was used to measure reactive oxygen species production and 3-(4,5-dimethylthiazol-2-yl)-2,5-diphenyltetrazolium bromide was used to measure cell viability. The results of the present study demonstrated that exposure to HG increased apoptosis and ROS production in HPMCs, whereas pretreatment with 1,25(OH)₂D₃ significantly inhibited HG-induced apoptosis and ROS production. Further analysis revealed that 1,25(OH)₂D₃ facilitated cell survival via the MAPK/P38 pathway. The results of the present study indicate that 1,25(OH)₂D₃ inhibits apoptosis and ROS production in HG-induced HPMCs via inhibition of the MAPK/P38 pathway.

Introduction

Peritoneal dialysis (PD) is a common therapy for the treatment of patients with end-stage renal disease (ESRD). Traditional PD solutions containing high glucose (HG) are effective, inexpensive and easily metabolized. However, the disadvantages of glucose-based solutions include reduced pH, increased lactate levels, the production of glucose degradation products and hyperosmolarity (1,2). Eventually, these changes may result in damage to the structure and function of the peritoneal membrane, leading to ultrafiltration failure and peritoneal fibrosis.

Apoptosis, also termed programmed cell death, generally occurs via two basic pathways; the intrinsic and extrinsic pathways. The B-cell lymphoma-2 (Bcl-2) gene family is associated with the gene-regulated, intrinsic pathway. Two important proteins of this family are Bcl-2 and Bcl-2-associated X protein (Bax), which are anti- and proapoptotic, respectively (3). Apoptosis is essential for the maintenance of normal homeostasis; however, when the physiological rate of apoptosis changes it can lead to disease (4). It has previously been demonstrated that HG can induce apoptosis in peritoneal mesothelial cells (5). This effect on peritoneal homeostasis may induce failure of peritoneal membrane function (6,7). It is well established that HG can cause mitochondrial oxidative stress. Overproduction of reactive oxygen species (ROS), driven by HG metabolism, can trigger cell death by modulating a series of intracellular signaling pathways (5). Therefore, understanding the regulation of apoptosis and oxidative stress may be important for PD therapy.

The effects of 1,25(OH)₂D₃ and its analogues have previously been investigated on the regulation of cell immunomodulation, proliferation and differentiation (8), and a previous study demonstrated that 1,25(OH)₂D₃ modulates apoptosis (9). In addition, research has demonstrated that vitamin D decreases ROS generation in HG-exposed monocytes (10). Various molecular pathways have been suggested to mediate protective and antioxidative effects against cell death, including inhibition of glycogen synthase kinase-3 and phosphoinositide phosphatases, enhanced activity of cell survival molecules (such as Bcl-2), and decreased activity of proapoptotic molecules, including Bax, mitogen-activated protein

Correspondence to: Professor Jianfei Ma, Department of Nephrology, The First Affiliated Hospital, China Medical University, 155 Nanjing North Street, Shenyang, Liaoning 110001, P.R. China
E-mail: majianfei56@sohu.com

Abbreviations: HPMCs, human peritoneal mesothelial cells; HG, high glucose; ROS, reactive oxygen species; PD, peritoneal dialysis; ESRD, end-stage renal disease; DCF-DA, dichlorofluorescein diacetate; MAPK, mitogen-activated protein kinase

Key words: human peritoneal mesothelial cells, apoptosis, 1,25(OH)₂D₃, reactive oxygen species, P38 mitogen-activated protein kinase, high glucose

kinase (MAPK)8 (also termed JNK) and P38 MAPK (11,12). The importance of MAPK proteins in human peritoneal mesothelial cells (HPMCs) during HG-induced oxidative stress and apoptosis remains unclear. The aim of the present study was to evaluate whether 1,25(OH)₂D₃ protects HPMCs from HG-induced apoptosis and oxidative stress, and to elucidate the molecular mechanisms involved.

Materials and methods

Materials. Fetal bovine serum (FBS) and penicillin-streptomycin were obtained from Gibco; Thermo Fisher Scientific, Inc. (Waltham, MA, USA). 1,25(OH)₂D₃ and dimethyl sulfoxide (DMSO) were purchased from Sigma-Aldrich (St. Louis, MO, USA). Rabbit polyclonal phosphorylated (p)-P38 (cat. no. sc-7975-R), rabbit polyclonal P38 (cat. no. sc-535) and mouse monoclonal β -actin (cat. no. sc-47778) antibodies were purchased from Santa Cruz Biotechnology, Inc. (Dallas, TX, USA). Rabbit monoclonal Bax (cat. no. 5023) and rabbit polyclonal Bcl-2 (cat. no. 2876) antibodies were purchased from Cell Signaling Technology, Inc. (Danvers, MA, USA). SB203580 (P38 MAPK inhibitor) was obtained from Selleck Chemicals (Houston, TX, USA). Annexin V/fluorescein isothiocyanate (FITC) Apoptosis Detection kit I was obtained from BD Pharmingen (San Diego, CA, USA). Enhanced chemiluminescence (ECL) kit was obtained from Pierce Biotechnology, Inc. (Rockford, IL, USA). The fluorescence microplate reader (ELx-800) was from Bio-Tek Instruments, Inc. (Winooski, VT, USA) and FACSCalibur flow cytometer was from BD Biosciences (Franklin Lakes, NJ, USA). An inverted microscope (Eclipse Ti; Nikon Corporation, Tokyo, Japan) was used to detect morphological changes.

HPMC culture. HPMCs (originally established by Dr Pierre Ronco, Department of Nephrology, Tenon Hospital, Paris, France) were provided by Professors Na Di and Xu Huimian (The First Affiliated Hospital of China Medical University, Shenyang, China) and cultured in RPMI-1640 medium (Hyclone; GE Healthcare Life Sciences, Logan, UT, USA) supplemented with 10% FBS. HPMCs were incubated in a 5% CO₂ atmosphere at 37°C, and the culture medium was changed every 2-3 days. HPMCs were detached using trypsin-EDTA with a subcultivation ratio between 1:3 and 1:4. Cells at passage 5-10 were used in all experiments. The HPMCs were divided into the following four treatment groups: i) Control group; ii) 1,25(OH)₂D₃ group, cells received 10⁻⁷ mol/l 1,25(OH)₂D₃ treatment for 24 h (9); iii) HG (Sinopharm Chemical Reagent Co., Ltd., Shanghai, China) group, cells received 126 mM HG treatment for 24 h; and iv) HG + 1,25(OH)₂D₃ group, cells received 10⁻⁷ mol/l 1,25(OH)₂D₃ pretreatment followed by 126 mM HG for 24 h. To investigate the MAPK/P38 signaling pathway, HPMCs were also incubated with 10 μ M SB203580 for 1 h and exposed to 126 mM HG in the presence of 10⁻⁷ mol/l 1,25(OH)₂D₃ for 24 h.

Measurement of cell viability. HPMCs were exposed to varying doses (76, 126 and 214 mM) of HG with or without pretreatment with different doses (10⁻⁸, 10⁻⁷ and 10⁻⁶ mol/l) of 1,25(OH)₂D₃ to observe the cell viability. Viability of HPMCs cultured in 96-well plates was measured using

3-(4,5-dimethylthiazol-2-yl)-2,5-diphenyltetrazolium bromide (MTT) assay. Briefly, following a 24-h incubation subsequent to treatment with HG and/or 1,25(OH)₂D₃, 10 μ l MTT (500 μ g/ml) was added to the culture medium and incubated at 37°C for 4 h. Subsequently, the supernatant was removed and 100 μ l DMSO was added to each well and mixed for 15 min. The absorbance value of the wells was measured at 570 nm using the microplate reader. The cell viability was expressed as the ratio of the signal obtained from treated and control groups.

Analysis of apoptosis. Apoptosis was assessed by FACSCalibur flow cytometry using the Annexin V/FITC Apoptosis Detection kit I, according to the manufacturer's protocol. HPMCs were cultured at 4x10⁶ cells/ml density and seeded in 6-well plates. Cells were trypsinized, then washed twice with cold phosphate-buffered saline (PBS) and centrifuged at 192 x g for 5 min. Cells were resuspended in 300 μ l 1X binding buffer, then 10 μ l Annexin V/FITC was added and incubated for 30 min at room temperature in the dark. Subsequently, 5 μ l propidium iodide was added to the cells in the dark. Finally, cells were analyzed by flow cytometry using WinMDI 2.8 software (The Scripps Institute, La Jolla, CA, USA) was used to analyze flow cytometry. Fluorescence-activated cell sorting data were used to determine the percentage of apoptotic cells.

Assessment of intracellular ROS levels. Intracellular accumulation of ROS was measured using 2,7-dichlorofluorescein diacetate (DCF-DA; Beijing Solarbio Science & Technology Co., Ltd., Beijing, China). HPMCs were seeded in 24-well plates and pretreated with 1,25(OH)₂D₃ for 2 h then exposed to HG for 24 h. The medium was then removed, cells were washed with PBS and incubated with DCF-DA for 30 min, then washed again with PBS. DCF oxidation was measured at 485 nm excitation and 525 nm emission wavelengths using the fluorescence microplate reader.

Western blot analysis. HPMCs were washed with PBS, incubated with radioimmunoprecipitation assay lysis buffer and the protein concentrations were quantified. Protein concentrations were quantified by BCA Protein assay (Pierce Biotechnology, Inc.). Each protein sample (50 μ g) was separated by 10% sodium dodecyl sulfate-polyacrylamide gel electrophoresis and was transferred onto a nitrocellulose membrane at 100 V for 60 min. The membranes were subsequently blocked in blocking solution (5% non-fat dry milk) for 1 h at room temperature, and were incubated overnight at 4°C with Bax, Bcl-2, P38, p-P38 or β -actin antibodies (1:1,000). Subsequently, each membrane was rinsed three times with Tris-buffered saline 0.1% Tween 20 (TBS-T) solution, then incubated with goat anti-rabbit IgG (cat. no. sc-2004; Santa Cruz Biotechnology, Inc.) and goat anti-mouse IgG (cat. no. sc-2005; Santa Cruz Biotechnology, Inc.) for 60 min at room temperature (dilution, 1:10,000). The membranes were washed with TBS-T solution, and an enhanced chemiluminescent western blotting detection system was used to detect specific signals. The band densities were measured using ImageJ software v1.6.0 (National Institutes of Health, Bethesda, Maryland, USA) and results were normalized against the reference gene β -actin.

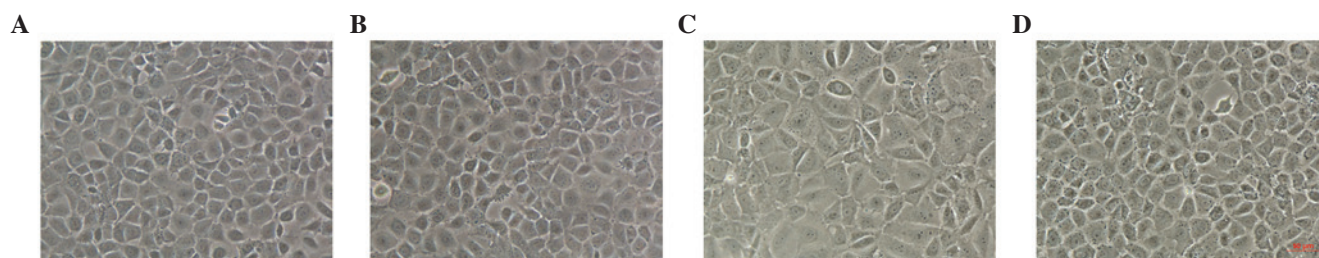


Figure 1. Morphological changes in cultured HPMCs. Representative images were captured of (A) the control group, (B) $1,25(\text{OH})_2\text{D}_3$ (10^{-7} mol/l) group, (C) HG group and (D) HG + $1,25(\text{OH})_2\text{D}_3$ (10^{-7} mol/l) group. Magnification, x200. Control HPMCs exhibited a cobblestone-like appearance, whereas the cells treated with HG displayed a fibroblast-like morphology. Treatment with $1,25(\text{OH})_2\text{D}_3$ (10^{-7} mol/l) attenuated the changes in cell morphology induced by HG. HPMC, human peritoneal mesothelial cell; HG, high glucose.

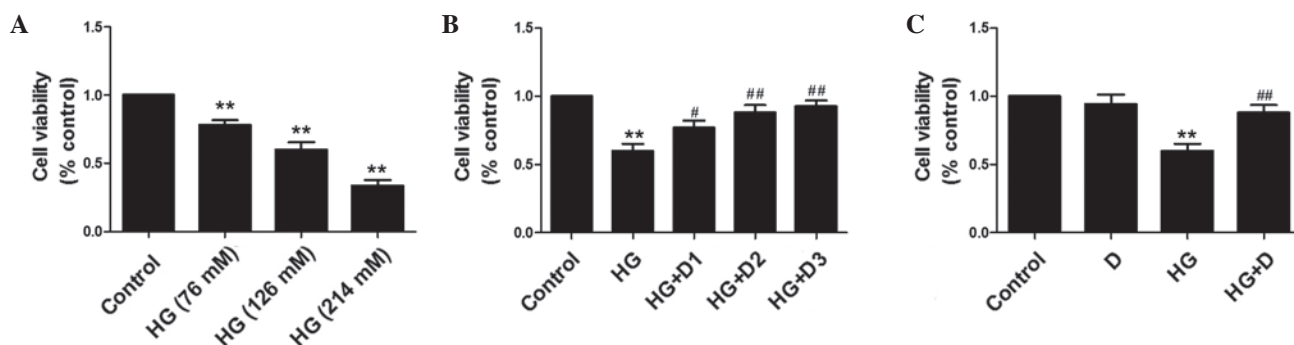


Figure 2. Effects of $1,25(\text{OH})_2\text{D}_3$ on cell viability in HG-treated human peritoneal mesothelial cells. The cell viability was analyzed by MTT assay. (A) Cells were exposed to HG at 76, 126 or 214 mM. (B) Cells were exposed to HG (126 mM) and pretreated with 10^{-8} , 10^{-7} or 10^{-6} mol/l $1,25(\text{OH})_2\text{D}_3$. (C) Cells were exposed to HG (126 mM) and pretreated with 10^{-7} mol/l $1,25(\text{OH})_2\text{D}_3$. Data are presented as the mean \pm standard error, n=6. **P<0.01 vs. control, #P<0.05 vs. HG, ##P<0.01 vs. HG. HG, high glucose; D, $1,25(\text{OH})_2\text{D}_3$; D1, 10^{-8} mol/l, D2, 10^{-7} mol/l; D3, 10^{-6} mol/l.

Statistical analysis. Statistical analysis was performed using SPSS software (version 18; SPSS, Inc., Chicago, IL, USA). Data are expressed as the mean \pm standard error. Multiple group comparisons were made using standard one-way analysis of variance methodology and individual comparisons were performed using Tukey's multiple comparison test. P<0.05 was considered to indicate a statistically significant difference.

Results

Morphological alterations of HPMCs. The control HPMCs exhibited a characteristic cobblestone-like appearance, which was changed to a fibroblast-like morphology after 24 h of incubation with HG (Fig. 1). Treatment with $1,25(\text{OH})_2\text{D}_3$ (10^{-7} mol/l) reversed the changes in cell morphology induced by HG. However, $1,25(\text{OH})_2\text{D}_3$ alone had no effect on the morphological characteristics of HPMCs (Fig. 1).

Effects of $1,25(\text{OH})_2\text{D}_3$ on cell viability in HG-stimulated HPMCs. To investigate the growth inhibitory effects of HG on HPMCs, cell viability was measured following treatment with different doses of HG (76, 126 and 214 mM) and $1,25(\text{OH})_2\text{D}_3$ (10^{-8} , 10^{-7} and 10^{-6} mol/l). Representative doses of 126 mM HG and 10^{-7} mol/l $1,25(\text{OH})_2\text{D}_3$ were chosen. Cells were stimulated with HG (126 mM) for 24 h, in the presence or absence of $1,25(\text{OH})_2\text{D}_3$ (10^{-7} mol/l). Cell viability was detected by MTT analysis. As demonstrated in Fig. 2A, HG significantly inhibited cell viability in HPMCs in a dose-dependent manner

(P<0.01). However, pretreatment with $1,25(\text{OH})_2\text{D}_3$ improved cell viability in a dose-dependent manner (Fig. 2B and C).

Effects of $1,25(\text{OH})_2\text{D}_3$ on HG-induced apoptosis in HPMCs. To assess the mechanisms by which $1,25(\text{OH})_2\text{D}_3$ alters HG-induced apoptosis in HPMCs, cell apoptosis was detected by FACSCalibur flow cytometry following Annexin V/PI double staining. FACSCalibur flow cytometry assays demonstrated that treatment with HG for 24 h markedly increased the level of apoptotic and dead cells detected. Treatment with $1,25(\text{OH})_2\text{D}_3$ markedly decreased the population of apoptotic and dead cells (Fig. 3A).

To further investigate the effects of $1,25(\text{OH})_2\text{D}_3$ on HG-induced apoptosis, western blot analysis was conducted to detect Bax and Bcl-2 levels. As demonstrated in Fig. 3B and C, HG upregulated the expression of Bax (P<0.01) and downregulated the expression of Bcl-2 (P<0.01) compared with control cells. Compared with the HG-treated cells, HG-induced apoptosis was attenuated by pretreatment of HPMCs with 10^{-7} mol/l $1,25(\text{OH})_2\text{D}_3$.

Effects of $1,25(\text{OH})_2\text{D}_3$ on intracellular ROS production in HG-treated HPMCs. It has previously been demonstrated that ROS contribute to HG-induced apoptosis in rat PMCs (RPMCs) (5). The aim of the present study was to demonstrate whether $1,25(\text{OH})_2\text{D}_3$ influences the elevated expression of ROS in HG-treated HPMCs. ROS levels were detected using DCF-DA. As demonstrated in Fig. 4, exposure to 126 mM glucose for 24 h increased the DCF signal compared with the

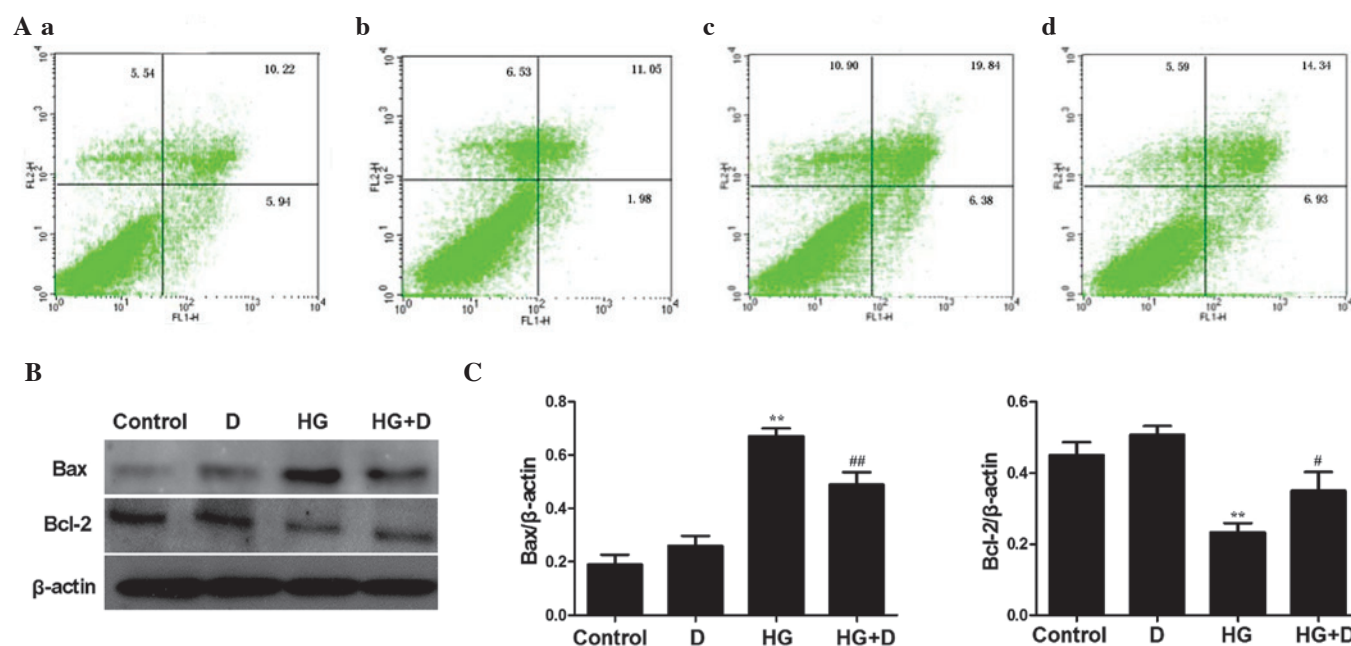


Figure 3. Effects of 1,25(OH)₂D₃ on HG-induced apoptosis in human peritoneal mesothelial cells. Cells were exposed to HG (126 mM), 10⁻⁷ mol/l 1,25(OH)₂D₃ or both for 24 h. (A) The levels of apoptosis were determined by Annexin V-propidium iodide double staining and flow cytometry: Top left quadrant, necrotic cells; lower left, normal cells; top right, early apoptotic cells; lower right, late apoptotic cells. (a) Control group; (b) 1,25(OH)₂D₃ (10⁻⁷ mol/l) group; (c) HG group; (d) HG + 1,25(OH)₂D₃ (10⁻⁷ mol/l) group. Flow cytometry assays demonstrated a marked increase in apoptotic (26.22%) and necrotic (10.90%) cells treated with HG for 24 h. However, 1,25(OH)₂D₃ pretreatment significantly decreased the population of apoptotic (21.27%) and necrotic (5.59%) cells. (B) Western blot analysis was performed and the (C) relative expression levels of Bax and Bcl-2 were calculated using densitometric analysis and were normalized to the loading control. Data are presented as the mean ± standard error of the relative intensities, n=3. **P<0.01 vs. control, #P<0.05 and ##P<0.01 vs. HG. HG, high glucose; D, 1,25(OH)₂D₃; Bax, Bcl-2-associated X protein; Bcl-2, B-cell lymphoma 2.

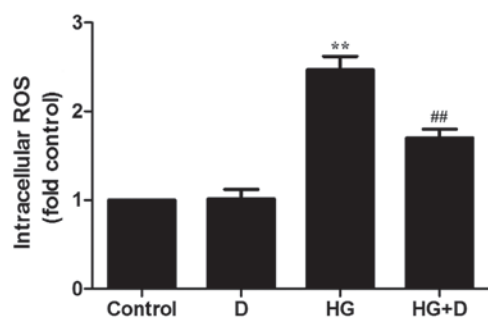


Figure 4. Effects of 1,25(OH)₂D₃ on HG-induced ROS generation in human peritoneal mesothelial cells. Cells were pretreated with 1,25(OH)₂D₃ for 2 h, then exposed to HG (126 mM) for 24 h, and intracellular ROS levels were measured. Data are presented as the mean ± standard error, n=6. **P<0.01 vs. control, ##P<0.01 vs. HG. D, 1,25(OH)₂D₃; HG, high glucose; ROS, reactive oxygen species.

control group (P<0.01). However, compared with HG-induced levels, pretreatment with 10⁻⁷ mol/l 1,25(OH)₂D₃ inhibited increases to ROS levels (P<0.01), as measured by DCF fluorescence.

Effects of 1,25(OH)₂D₃ on the MAPK/P38 pathway in HG-treated HPMCs. MAPKs are associated with various biological activities, including cell proliferation, differentiation, survival, transformation, and cell death (13,14). Extracellular-regulated kinase (ERK), P38 and JNK are three important members of the MAPK family. To investigate the molecular mechanism by which 1,25(OH)₂D₃ exerts its

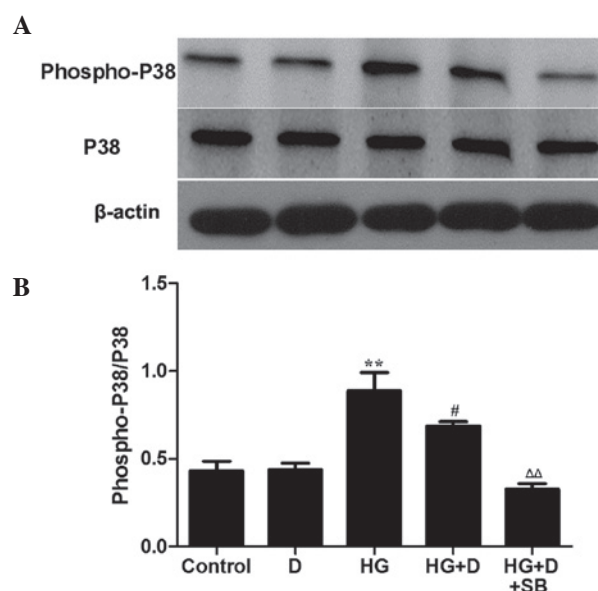


Figure 5. Effects of 1,25(OH)₂D₃ on the MAPK/P38 pathway in HG-treated HPMCs. HPMCs were incubated with or without 10 μM SB203580 for 1 h and then exposed to HG (126 mM) in the presence or absence of 10⁻⁷ mol/l 1,25(OH)₂D₃. (A) Western blot analysis was performed to detect P38 and phospho-P38. (B) The protein levels were assessed using densitometry and are expressed as relative intensities. Data are presented as the mean ± standard error, n=3. **P<0.01 vs. control, #P<0.05 vs. HG, ^{ΔΔ}P<0.01 vs. HG + D. HPMC, human peritoneal mesothelial cell; MAPK, mitogen-activated protein kinase; P38, MAPK 14; D, 1,25(OH)₂D₃; HG, high glucose; SB, SB203580.

anti-apoptotic effects, the MAPK/P38 pathway was examined. HPMCs were incubated with or without 10 μM SB203580 for

1 h and were then exposed to 126 mM HG in the presence or absence of 10^{-7} mol/l $1,25(\text{OH})_2\text{D}_3$. P38 activation was detected by western blot analysis using a p-P38 antibody. When cells were exposed to HG alone, P38 phosphorylation was increased compared with the control ($P < 0.01$), whereas phosphorylation was significantly decreased by $1,25(\text{OH})_2\text{D}_3$ treatment compared with HG ($P < 0.05$; Fig. 5). In addition, treatment of HG-stimulated HPMCs with SB203580 and $1,25(\text{OH})_2\text{D}_3$ inhibited P38 phosphorylation to a greater extent compared with $1,25(\text{OH})_2\text{D}_3$ treatment ($P < 0.01$; Fig. 5). These results suggest that $1,25(\text{OH})_2\text{D}_3$ protects HPMCs through the MAPK/P38 pathway.

Discussion

When the peritoneum is continuously exposed to HG the structure and function of the peritoneal membrane is altered. HG may lead to increased peritoneal permeability, resulting in rapid dissipation of the osmotic gradient, eventually causing ultrafiltration failure and inadequate dialysis (15). The present study demonstrated that HG significantly inhibits the cell viability of HPMCs, and alters the cell morphology. However, $1,25(\text{OH})_2\text{D}_3$ enhanced the viability of HPMCs and reversed the observed changes to cell morphology induced by HG.

It has previously been demonstrated that $1,25(\text{OH})_2\text{D}_3$ decreases apoptosis in RPMCs (9). Plasma levels of $1,25(\text{OH})_2\text{D}_3$ have been observed to be reduced in patients with ESRD. Therefore, it was hypothesized that $1,25(\text{OH})_2\text{D}_3$ may affect apoptosis in HPMCs. The $1,25(\text{OH})_2\text{D}_3$ concentration used in the present study was selected according to MTT assay results and a previous investigation (9). The present study investigated the effects of $1,25(\text{OH})_2\text{D}_3$ on HG-induced apoptosis in HPMCs and aimed to elucidate the molecular mechanisms involved. It was demonstrated that pretreatment with $1,25(\text{OH})_2\text{D}_3$ decreased the ratio of Bax/Bcl-2 protein expression and the rate of apoptosis induced by HG. These findings support the results of a previous study that demonstrated that $1,25(\text{OH})_2\text{D}_3$ inhibits podocyte apoptosis via downregulating Bax and upregulating Bcl-2 expression levels, which may result in improved podocytopenia (16).

Previous studies have demonstrated that HG induces apoptosis via the ROS signaling pathway, and evidence suggested that overproduction of ROS was associated with apoptotic cell death (17,18). The present study demonstrated that ROS production was increased by HG and that $1,25(\text{OH})_2\text{D}_3$ decreases HG-induced ROS production in HPMCs. In agreement with the findings of the present study, a previous study demonstrated that the protective activity of $1,25(\text{OH})_2\text{D}_3$ was mediated by antioxidant ROS inhibition and associated with reduced tumor necrosis factor- α and nuclear factor- κB levels (19). It has also been previously demonstrated that T cell apoptosis was mediated via ROS generation in response to the downregulation of vitamin D receptor (20). However, to the best of our knowledge, this is the first report demonstrating the protective role of $1,25(\text{OH})_2\text{D}_3$ against HG-induced apoptosis and ROS production in HPMCs.

Previous research has demonstrated that oxidative stress stimulates the phosphorylation of MAPKs, including P38, ERK1/2 and JNK1/2, which are important components of the signaling pathways associated with cell death (21-25).

The association between ROS and MAPK signaling remains unknown. It was previously demonstrated that ROS may activate apoptosis signal regulated kinase 1, a MAPK kinase that activates JNK and P38 (26). The results of the present study revealed that pretreatment with $1,25(\text{OH})_2\text{D}_3$, as an early signaling factor, inhibited HG-induced P38 phosphorylation. The results of the present study are in accordance with previous reports indicating that baicalein prevented apoptosis by reducing ROS generation and deactivating MAPK/ERK/JNK/P38 signaling pathways (27).

In conclusion, the results of the present study revealed that in HG-stimulated HPMCs, $1,25(\text{OH})_2\text{D}_3$ attenuated changes to cell morphology, and reduced apoptosis and ROS production, partially mediated by inhibition of the MAPK/P38 pathway. The results of the present study suggested that $1,25(\text{OH})_2\text{D}_3$ may be employed in the future as a promising therapeutic agent for the prevention or treatment of peritoneal damage.

Acknowledgements

The present study was supported by the National Natural Science Foundation of China (grant no. 81300636).

References

1. Mortier S, De Vriese AS and Lameire N: Recent concepts in the molecular biology of the peritoneal membrane - implications for more biocompatible dialysis solutions. *Blood Purif* 21: 14-23, 2003.
2. Ahmad M, Shah H, Pliakogiannis T and Oreopoulos DG: Prevention of membrane damage in patient on peritoneal dialysis with new peritoneal dialysis solutions. *Int Urol Nephrol* 39: 299-312, 2007.
3. Ghibelli L and Diederich M: Multistep and multitask Bax activation. *Mitochondrion* 10: 604-613, 2010.
4. Ortiz A: Nephrology forum: Apoptotic regulatory proteins in renal injury. *Kidney Int* 58: 467-485, 2000.
5. Zhang X, Liang D, Guo B, Yang L, Wang L and Ma J: Zinc inhibits high glucose-induced apoptosis in peritoneal mesothelial cells. *Biol Trace Elem Res* 150: 424-432, 2012.
6. Zheng ZH, Ye RG, Bergström J and Lindholm B: Effect of dialysate composition on the apoptosis and proliferation of human peritoneal mesothelial cells and protein expression of Fas and c-Myc. *Adv Perit Dial* 16: 31-35, 2000.
7. Kaifu K, Kiyomoto H, Hitomi H, Matsubara K, Hara T, Moriwaki K, Ihara G, Fujita Y, Sugawara N, Nagata D, *et al*: Insulin attenuates apoptosis induced by high glucose via the PI3-kinase/Akt pathway in rat peritoneal mesothelial cells. *Nephrol Dial Transplant* 24: 809-815, 2009.
8. Gocek E, Kiełbiński M, Wyłób P, Kutner A and Marcinkowska E: Side-chain modified vitamin D analogs induce rapid accumulation of VDR in the cell nuclei proportionately to their differentiation-inducing potential. *Steroids* 73: 1359-1366, 2008.
9. Yang L, Wang J, Fan Y, Chen S, Wang L and Ma J: Effect of $1,25(\text{OH})_2\text{D}_3$ on rat peritoneal mesothelial cells treated with high glucose plus lipopolysaccharide. *Cell Immunol* 271: 173-179, 2011.
10. Jain SK and Micinski D: Vitamin D upregulates glutamate cysteine ligase and glutathione reductase, and GSH formation, and decreases ROS and MCP-1 and IL-8 secretion in high-glucose exposed U937 monocytes. *Biochem Biophys Res Commun* 437: 7-11, 2013.
11. Chiu CT and Chuang DM: Molecular actions and therapeutic potential of lithium in preclinical and clinical studies of CNS disorders. *Pharmacol Ther* 128: 281-304, 2010.
12. Kim YH, Rane A, Lussier S and Andersen JK: Lithium protects against oxidative stress-mediated cell death in α -synuclein-overexpressing in vitro and in vivo models of Parkinson's disease. *J Neurosci Res* 89: 1666-1675, 2011.

13. McCubrey JA, Lahair MM and Franklin RA: Reactive oxygen species-induced activation of the MAP kinase signaling pathways. *Antioxid Redox Signal* 8: 1775-1789, 2006.
14. Kholodenko BN and Birtwistle MR: Four-dimensional dynamics of MAPK information processing systems. *Wiley Interdiscip Rev Syst Biol Med* 1: 28-44, 2009.
15. Jörres A and Witowski J: PD membrane: Biological responses to different PD fluids. *Contrib Nephrol* 150: 48-53, 2006.
16. Zou MS, Yu J, Nie GM, He WS, Luo LM and Xu HT: 1, 25-dihydroxyvitamin D₃ decreases adriamycin-induced podocyte apoptosis and loss. *Int J Med Sci* 7: 290-299, 2010.
17. Greene DA, Stevens MJ, Obrosova I and Feldman EL: Glucose-induced oxidative stress and programmed cell death in diabetic neuropathy. *Eur J Pharmacol* 375: 217-223, 1999.
18. Lelkes E, Unsworth BR and Lelkes PI: Reactive oxygen species, apoptosis and altered NGF-induced signaling in PC12 pheochromocytoma cells cultured in elevated glucose: An in vitro cellular model for diabetic neuropathy. *Neurotox Res* 3: 189-203, 2001.
19. Lan N, Luo G, Yang X, , Cheng Y, Zhang Y, Wang X, Wang X, Xie T, Li G, Liu Z and Zhong N: 25-Hydroxyvitamin D₃-deficiency enhances oxidative stress and corticosteroid resistance in severe asthma exacerbation. *PLoS One* 9: e111599, 2014.
20. Rehman S, Chandel N, Salhan D, Rai P, Sharma B, Singh T, Husain M, Malhotra A and Singhal PC: Ethanol and vitamin D receptor in T cell apoptosis. *J Neuroimmune Pharmacol* 8: 251-261, 2013.
21. Raman M, Chen W and Cobb MH: Differential regulation and properties of MAPKs. *Oncogene* 26: 3100-3112, 2007.
22. Liu B, Jian Z, Li Q, Li K, Wang Z, Liu L, Tang L, Yi X, Wang H, Li C and Gao T: Baicalein protects human melanocytes from H₂O₂-induced apoptosis via inhibiting mitochondria-dependent caspase activation and the p38 MAPK pathway. *Free Radic Biol Med* 53: 183-193, 2012.
23. Lee HJ, Noh YH, Lee DY, Kim YS, Kim KY, Chung YH, Lee WB and Kim SS: Baicalein attenuates 6-hydroxydopamine-induced neurotoxicity in SH-SY5Y cells. *Eur J Cell Biol* 84: 897-905, 2005.
24. Chen YC, Chow JM, Lin CW, Wu CY and Shen SC: Baicalein inhibition of oxidative-stress-induced apoptosis via modulation of ERKs activation and induction of HO-1 gene expression in rat glioma cells C6. *Toxicol Appl Pharmacol* 216: 263-273, 2006.
25. Lin HY, Shen SC, Lin CW, Yang LY and Chen YC: Baicalein inhibition of hydrogen peroxide-induced apoptosis via ROS-dependent heme oxygenase 1 gene expression. *Biochim Biophys Acta* 1773: 1073-1086, 2007.
26. Nagai H, Noguchi T, Takeda K and Ichijo H: Pathophysiological roles of ASK1-MAP kinase signaling pathways. *J Biochem Mol Biol* 40: 1-6, 2007.
27. Chen HM, Hsu JH, Liou SF, Chen TJ, Chen LY, Chiu CC and Yeh JL: Baicalein, an active component of *Scutellaria baicalensis* Georgi, prevents lysophosphatidylcholine-induced cardiac injury by reducing reactive oxygen species production, calcium overload and apoptosis via MAPK pathways. *BMC Complement Altern Med* 14: 233, 2014.